

Atomic layer etching of silicon dioxide using alternating C₄F₈ and energetic Ar⁺ plasma beams

Sanbir S Kaler, Qiaowei Lou, Vincent M Donnelly and Demetre J Economou

Department of Chemical and Biomolecular Engineering, Plasma Processing Laboratory, University of Houston, Houston, TX 77204, United States of America

E-mail: vmdonnelly@uh.edu and economou@uh.edu

Received 14 February 2017, revised 19 April 2017

Accepted for publication 25 April 2017

Published 16 May 2017



Abstract

Atomic layer etching (ALE) of SiO₂ was studied by alternating exposure of a 5 nm-thick SiO₂ film on Si substrate to (1) a plasma beam emanating from a c-C₄F₈ inductively coupled plasma (ICP), to grow a fluorocarbon (FC) film composed mainly of CF₂, and (2) an energetic (130 eV) Ar⁺ ion beam extracted from a separate Ar ICP. *In situ* x-ray photoelectron spectroscopy was used to analyze the chemical composition of the near-surface region, and to quantify the thickness of the FC and SiO₂ films. A very thin (3–6 Å), near self-limiting thickness CF₂-rich FC film was found to deposit on the SiO₂ surface with exposure to continuous or pulsed power C₄F₈ plasma beams, under conditions that generated a large relative flux of CF₂. Following this, a FC film of similar composition grew at ~10 times slower rate. Exposure of the thin film to the Ar⁺ beam led to removal of 1.9 Å SiO₂. An estimated yield of 1.3 SiO₂ molecules-per-Ar⁺ was found for a single ALE step. The rate of 1.9 Å/cycle persisted over multiple ALE cycles, but a carbon-rich residual film did build up. This film can be removed by a brief exposure to an O₂-containing plasma beam.

Keywords: atomic layer etching, silicon dioxide, argon ion beam, fluorocarbon plasma, fluorocarbon film, quasi self-limiting

(Some figures may appear in colour only in the online journal)

1. Introduction

Fabrication of devices with feature sizes 10 nm and below requires manufacturing with atomic level precision [1, 2]. Atomic layer deposition (ALD) has been used successfully in the microelectronics industry to grow films with controlled thickness down to a monolayer. Atomic layer etching (ALE), the inverse of ALD, has recently received renewed attention for nano-device manufacturing [3, 4]. ALE was studied [5–14] starting in the late 1980s as a cyclic process encompassing four steps: (1) Exposure of a clean substrate to a reactant gas, and chemisorption of the gas on the surface. This process should be self-limiting, in the sense that chemisorption stops when all available surface sites are occupied. (2) Purging of excess reactant with an inert gas flow to avoid etching by gas-phase

species in the subsequent step. (3) Exposure of the surface to an energetic particle (e.g. ions, fast neutrals) beam, to effect reaction (e.g. chemical sputtering) between the adsorbed gas and the underlying solid. This process should also be self-limiting; ions should remove only substrate atoms bonded to the chemisorbed gas. Once this layer is removed, further etching (physical sputtering) of the substrate must not occur. (4) Evacuation of the chamber to exhaust the etching products. The cycle may be repeated to remove the desired number of layers. Athavale and Economou demonstrated atomic layer etching of silicon using Cl₂ gas and Ar⁺ ion bombardment through molecular dynamics (MD) simulations and experiments [15, 16], following the four steps enumerated above. MD results indicated a total silicon etching yield of 0.172 Si atoms removed per 50 eV Ar⁺. A dose of 1.16×10^{16} ions

cm^{-2} was required to remove one monolayer of silicon. The surface chlorination and ion bombardment steps were both self-limiting. Precise control of ion energy was deemed to be the most important factor in achieving removal of one monolayer/cycle. This early approach to ALE required a relatively long time (~ 100 s) per cycle, because no particular attention was paid to fast switching of gases, and reactor purging can be slow, especially when using gases such as Cl_2 that have a long residence time on the chamber walls.

A recent trend is to implement ALE in essentially 'standard' plasma etching reactors in which a continuous wave (cw) or a pulsed plasma of an inert gas (e.g. argon) is maintained. A short pulse of a reactive gas (e.g. Cl_2 for Si or C_4F_8 for SiO_2 ALE) is fed to the plasma leading to chemisorption or deposition of an extremely thin layer on the substrate surface. During this 'surface modification' step, the energy of ions bombarding the substrate is kept below the threshold for ion-assisted etching to avoid uncontrolled etching of the substrate. Subsequent exposure of the modified surface to an energetic particle (usually positive ion) flux causes reactions removing one or more of the top layers of the substrate. Bombardment of the substrate by energetic ions may be achieved by biasing the substrate holder. It is imperative that etching is highly selective, in the sense that the ions do not sputter the pristine substrate, after the modified layer has been removed. This requires ions with tight energy control. Also, deposition or growth of the surface modification layer should be self-limiting, so that the thickness of that layer is uniform across the substrate, regardless of non-uniformities of reactant flux to different areas of the substrate or variations of the aspect ratio of features. Self-limiting growth preserves the inherent uniformity of ALE, and also suppresses aspect ratio dependent etching (ARDE). Ideally, one cycle of reactant adsorption and subsequent reaction with the surface will remove a single monolayer of a substrate. In practice, more or less than a monolayer may be removed per cycle. This is acceptable as long as a controlled and precise amount of material is removed per cycle. Several complications can interfere with ALE [3, 4] making consistent layer-by-layer removal difficult or impossible. Examples include spontaneous chemical etching of the substrate (e.g. Cl atom etching of heavily n-doped poly-silicon [17]), photo-assisted etching [18], substrate sputtering, or excessive roughening of the surface.

Tan *et al* developed highly selective and directional ALE of silicon by using plasma assisted chlorine adsorption followed by Ar^+ ion-assisted etching in a commercial plasma etching chamber [19]. They measured the etching per cycle (EPC) while varying ion-energy. The 'ideal ALE process window' [3] for silicon was observed for Ar^+ energies in the 60–80 eV range, yielding an EPC ~ 14 Å of silicon. Within this window, the ion energy was high enough to remove the chlorinated silicon layer but not the bulk silicon underneath. For Ar^+ energy up to 70 eV the EPC for thermal silicon oxide was essentially zero, implying high selectivity of etching Si versus SiO_2 . Selectivity was explained by the difference in binding energies (6.4 eV for the Si–O bond versus 4.2 eV for Si–Cl), making replacement of O with Cl thermodynamically unfavorable.

Sherpa and Ranjan reported on the self-limiting, quasi-atomic layer etching of silicon nitride in a commercial capacitively coupled plasma reactor [20]. Two sequential steps per cycle were implemented: (1) surface modification in a hydrogen plasma, where hydrogen ions were implanted into silicon nitride upon applying a bias voltage on the substrate, and (2) removal of the modified layer in a fluorine-containing plasma. The silicon nitride EPC decreased with increasing number of ALE cycles, possibly due to accumulated structural damage on the surface. By adjusting the energy of the hydrogen ions implanted into the silicon nitride film, they successfully controlled an etched depth of 6 nm per cycle.

Atomic layer etching of SiO_2 using a fluorocarbon (FC) film as a surface modification layer was investigated computationally by Rauf *et al* [21] through molecular dynamics (MD) simulation, and by Agarwal and Kushner [22] using the hybrid plasma equipment model (HPM). Rauf *et al* studied deposition of a thin fluorocarbon film on oxide using low energy fluorocarbon ions (CF_2^+ and CF_3^+) and the subsequent removal of the top layer(s) of oxide via energetic Ar^+ ion bombardment. This two-step, layer-by-layer etching was successfully demonstrated in MD simulations by maintaining low ion energies during FC deposition and Ar^+ ion energies below 50 eV (physical sputtering threshold for SiO_2). Agarwal and Kushner studied ALE in a conventional plasma etcher, using an $\text{Ar}/\text{C}_4\text{F}_8$ mixture during both the deposition of the surface modification layer and etching steps, with a non-sinusoidal substrate bias waveform to limit the spread of the ion energy distribution [22]. The ion energy was carefully controlled to achieve selectivity.

Metzler *et al* studied layer-by-layer etching of SiO_2 using a cw argon plasma with periodic injection of a controlled number of C_4F_8 molecules, and synchronized Ar^+ ion bombardment with ion energies below the threshold for sputtering SiO_2 [4, 23]. With an argon plasma ignited, a small amount of fluorocarbon gas (1.5 s pulse of C_4F_8) was injected to deposit a 4–8 Å-thick FC film, followed by a 10 s period of no bias, where no etching or deposition occurred, followed by a 35 s period in which the substrate electrode was biased, allowing Ar^+ ions to bombard the modified SiO_2 surface, removing approximately 2.5 Å of SiO_2 per cycle for maximum ion energy of 25 eV. In another study by adjusting process parameters such as ion energy, etch step duration, and fluorocarbon film thickness, selective etching of SiO_2 to Si_3N_4 was achieved [24].

In this work, atomic layer etching of SiO_2 was studied with half steps consisting of deposition of a self-limiting FC film, composed mainly of CF_2 , followed by Ar^+ ion-bombardment, to remove a precise amount of SiO_2 . In contrast to recent ALE studies, the substrate was not immersed in the plasma; instead, the substrate was exposed sequentially to one of two plasma beams emanating from separate inductively coupled plasma (ICP) sources. Specifically, during FC film growth, the substrate was exposed to a plasma beam emanating from a $\text{c-C}_4\text{F}_8$ ICP source. During Ar^+ ion bombardment, the substrate was exposed to an ion beam extracted from an Ar ICP source. The Ar^+ ion energy was controlled by applying a bias voltage on a 'boundary electrode', in contact with the Ar plasma, and/or on the metallic substrate holder. *In situ* x-ray photoelectron

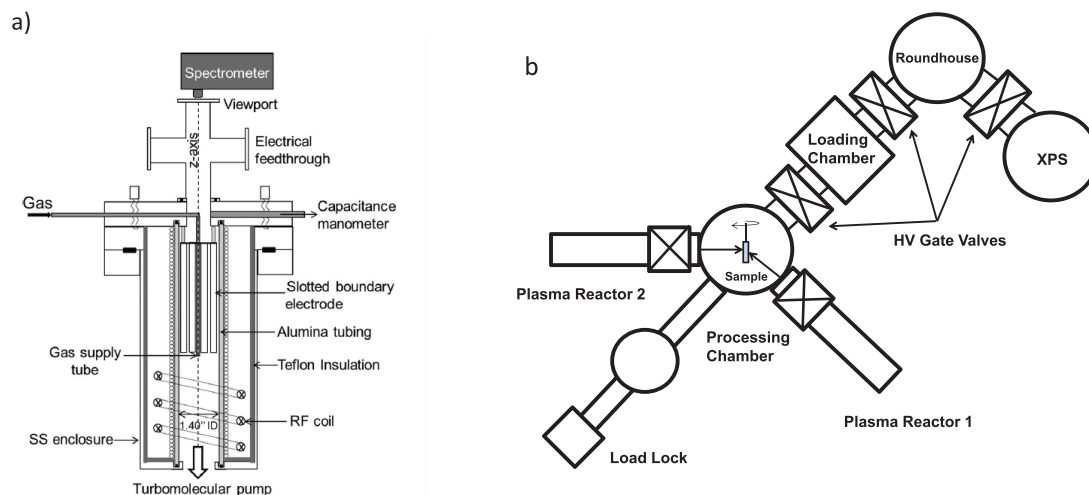


Figure 1. (a) Schematic of inductively coupled plasma (ICP) reactor. (b) Top view of the overall experimental system consisting of processing chamber, loading chamber, two ICP plasma reactors, and roundhouse with access to XPS.

spectroscopy was used to analyze the chemical composition of the near-surface region and to quantify the thickness of the fluorocarbon and SiO_2 films.

2. Experimental

The overall apparatus (figure 1) consisted of a processing chamber with two compact, inductively coupled plasma (ICP) sources. Beams of neutral and charged species generated in these ICPs impinged on a substrate that was introduced to a processing chamber through a loadlock. This chamber was pumped by a 300 l s^{-1} turbomolecular pump (Ebara ET-600WS) backed by a dry pump (Edwards, iH80). The base pressure, typically $\sim 3.0 \times 10^{-8}$ Torr, was measured using an ion gauge (Varian, model XGS-600). The processing chamber was also connected to an analysis chamber, allowing XPS to be performed without air exposure.

Each ICP reactor (figure 1(a)) consisted of a 3.56 cm inner diameter alumina tube, surrounded by a 3 turn antenna, made of 1/4" outer diameter copper tubing, and housed in a 4" outer diameter coaxial stainless steel cylindrical enclosure. Deionized cooling water flowed through the ICP coil and through Teflon tubing wrapped around the exterior wall of the alumina tube. A chiller maintained the water temperature at 20°C . Gas was fed into the reactor through a 1/4" stainless steel tube which was connected to a gas manifold. Flows of Ar, O_2 , or C_4F_8 were controlled by mass flow controllers (MKS model 1179A). One ICP reactor was used for deposition of fluorocarbon (FC) films and the second ICP reactor was used for Ar^+ beam irradiation of the sample. Power (13.56 MHz) to either ICP source was supplied by a Hewlett-Packard (model 3325A) waveform generator, and an ENI (model A-300) radio frequency power amplifier. Using an impedance matching network, the desired forward power could be delivered with essentially zero reflected power. Both forward and reflected powers were measured with in-line Bird-meters. Nearly mono-energetic Ar^+ ions with a narrow (few eV) energy spread were obtained by

applying a synchronous positive DC bias to a 'boundary electrode', in contact with the plasma, during the afterglow of a pulsed argon plasma [25]. The Ar pulsed ICP was operated at a modulation frequency of 10 kHz and 20% duty cycle, at a peak (average) power of 600 (120) W. A negative or positive DC bias (Kepco model KLP 150-16 power supply) was also applied to the substrate holder, allowing ion energy to be increased, or decreased to the extent that ions were prevented from reaching the substrate. With a boundary bias of +100 V and substrate bias of -30 V , the ion energy was 130 eV. An ion current of $130 \mu\text{A}$ was measured over the 40 cm^2 substrate surface area, corresponding to an ion flux of $1.7 \times 10^{13} \text{ ions cm}^{-2} \text{ s}^{-1}$.

During exposure to a plasma beam, the sample was rotated to be perpendicular to the reactor axis, at a distance of 10 cm from the end of the ICP discharge tube. A 0.5 cm diam. aperture was used on the Ar^+ beam; no aperture was used with the C_4F_8 plasma source. The pressure in the processing chamber was 7.7×10^{-5} Torr when the Ar^+ beam ICP was operated at a pressure of 7.7 mTorr, and the pressure in the processing chamber was 2.3×10^{-3} Torr, nearly independent of plasma conditions, when the C_4F_8 ICP was operated at a pressure of 6.5 mTorr. The C_4F_8 pressure in the processing chamber was not corrected for the higher sensitivity of the ionization gauge (for this gas or its fragments), so the actual pressure is probably half the given value, or somewhat less.

The processing chamber (figure 1(b)), where the substrate was housed, was equipped with a Physical Electronics (Model 10-420) x-ray photoelectron spectrometer. Samples were introduced into a loading chamber between a 'roundhouse' and processing chamber. The XPS and roundhouse chambers were each pumped by a separate ion pump (Gamma Vacuum, Model Titan™ 300TV) achieving base pressures of 3.0×10^{-9} Torr. The loading chamber was purged with dry nitrogen when inserting or removing a sample. The substrate was moved between chambers (where each chamber could be isolated by gate valves) with transfer arms, without exposure to the atmosphere. After being transferred to the processing chamber, a fresh sample was cleaned by a continuous wave

(cw) O₂ plasma (300 W, 10 mTorr, using the ICP source for the Ar⁺ beam) for 10 s, to remove hydrocarbon contamination of the ‘as-received’ samples.

Following selected processing steps, the sample was transferred to the XPS chamber for quantitative chemical analysis of the near-surface region. Peaks of interest included Si(2*p*), C(1*s*), O(1*s*), and F(1*s*). Samples consisted of 5 nm thermally grown SiO₂ on Si wafers (provided by Lam Research Corp.) that were cleaved into 1.5 cm × 1.5 cm squares. XPS spectra were initially gathered to verify the SiO₂ thickness t_{SiO_2} using the following formula,

$$t_{\text{SiO}_2} = \lambda_{\text{SiO}_2} \sin \theta \cdot \ln \left[1 + \frac{3 \cdot I_{\text{SiO}_2}}{I_{\text{Si}}} \cdot \frac{\lambda_{\text{Si}}}{\lambda_{\text{SiO}_2}} \cdot \frac{n_{\text{Si}}}{n_{\text{SiO}_2}} \right]$$

where the λ_{SiO_2} and λ_{Si} are electron inelastic mean free paths of 3.8 nm and 2.2 nm in SiO₂ and Si, respectively [26–28]. θ is the angle between the sample surface and the axis of the photoelectron collection lens ($\theta = 90^\circ$). n_{SiO_2} and n_{Si} are the atom densities of SiO₂ ($6.92 \times 10^{22} \text{ cm}^{-3}$) and Si ($5.00 \times 10^{22} \text{ cm}^{-3}$) [28]. I_{SiO_2} and I_{Si} are the integrated intensities of SiO₂ (2*p*) and Si(2*p*) peaks, near 99.5 and 104 eV, respectively. The fluorocarbon film thickness, t_{FC} , was computed using,

$$t_{\text{FC}} = \lambda_{\text{FC}} \sin \theta \cdot \ln \left[1 + \frac{\frac{3I_{\text{FC}}}{n_{\text{FC}} \cdot S_{\text{C}} \cdot \lambda_{\text{FC}}}}{\frac{I_{\text{Si}}}{n_{\text{Si}} \cdot S_{\text{Si}} \cdot \lambda_{\text{Si}}} + \frac{3I_{\text{SiO}_2}}{n_{\text{SiO}_2} \cdot S_{\text{SiO}_2} \cdot \lambda_{\text{SiO}_2}}} \right]$$

where $\lambda_{\text{FC}} = 1.8 \text{ nm}$ and $n_{\text{FC}} = 7.95 \times 10^{22} \text{ cm}^{-3}$ are the electron inelastic mean free path and atom density (C plus F atoms per cm³), taken to be those of polytetrafluoroethylene, and I_{FC} is the integrated intensity of the C(1*s*) peak. $S_{\text{Si}} = 0.817$ and $S_{\text{C}} = 1$ are XPS sensitivity factors for Si(2*p*) and C(1*s*), respectively [26].

3. Results and discussion

One atomic layer etching cycle consisted of exposure of SiO₂ to a beam of fluorocarbon radicals and fluorine atoms generated in a c-C₄F₈ ICP, followed by product removal with an energetic Ar⁺ ion beam extracted from a second ICP. Each half-step was studied by XPS. Times required for pseudo-saturation of fluorocarbon (FC) film deposition and product removal were determined, and multiple ALE cycles were carried out with XPS analysis after a desired number of cycles.

3.1. Fluorocarbon film growth and fluorine uptake

XPS spectra of as-received samples revealed the peaks anticipated for Si in SiO₂ and in the underlying substrate at expected binding energies of 104.0 eV and 99.5 eV, as well as O(1*s*) at 533.0 eV, and C(1*s*) at 286.2 eV from air contamination. The hydrocarbon contamination was removed by exposing the sample to an O₂ plasma beam (300 W cw O₂ plasma at 10 mTorr) for 10 s. After this cleaning step, fluorocarbon films were deposited by exposing the sample for various times to the beam effusing from a c-C₄F₈ plasma, without any bias voltage applied. Figures 2(a) and (b) show C(1*s*) spectra for short (2 s, 6.3 Å-thick film) and long (180 s, 22.4 Å-thick

film) exposure to a c-C₄F₈ plasma beam by a 50 W cw ICP (10 sccm, 16 mTorr). Peaks at 287.3 eV, 289.6 eV, 292.0 eV, and 293.8 eV have previously been assigned to C–(CF_{*x*})_{*y*}, CF, CF₂, and CF₃, respectively, for fluorocarbon films [29, 30]. The FC film composition is virtually the same for the first few monolayers grown on SiO₂ and the bulk film, with CF₂ being the main component.

Figure 2(c) shows the F(1*s*) spectra for the same thin and thick films, along with a spectrum, labeled ‘SiF_{*x*}’, recorded after 18 s Ar⁺ ion bombardment following deposition by the C₄F₈ plasma. The peak position for the thick film is close to that reported for a Teflon-like film [29]. The F(1*s*) binding energy for the SiF_{*x*} film spectrum is consistent with that reported for F bound to Si [29], hence we attribute this fluorine component to F bound to Si in SiO₂. The binding energy for the thin film spectrum is between these two cases, suggesting F is bound to both C and Si. This is also confirmed by a comparison of the F-to-C stoichiometry determined from a deconvolution of the C(1*s*) with that derived from the F(1*s*)-to-C(1*s*) intensity ratio. The F-to-C ratios derived from the C(1*s*) peak deconvolution were similar for the 6.3 Å and 22.4 Å thick films (1.8 and 1.65, respectively). Conversely, the F-to-C ratio determined from the F(1*s*)-to-C(1*s*) ratio was much higher for the thin film, compared to that for the thick film (4.6 versus 2.6). Hence, for the thin film, only 39% of the fluorine was contained in the fluorocarbon film; the majority of F was instead in the SiO₂ layer, bound to Si. For the 22.4 Å film, the majority (63%) of F was in the fluorocarbon film. In still thicker films, nearly all of the detected F can be accounted for by the fluorocarbon film (e.g. 83% in a 58 Å thick film).

Figure 3(a) shows the fluorocarbon film thickness as a function of time, grown using the C₄F₈ plasma beam by a continuous wave 50 W ICP. Two deposition phases are observed: (1) a fast deposition rate, ascribed below to a relatively high probability for chemisorption of reactive species in the beam on the SiO₂ surface to form a near-saturated, 8 Å-thick layer after a relatively short time, and (2) a slower deposition rate, due to the much lower probability for chemisorption of species on the fluorocarbon film. The total atomic fluorine concentration in the near surface region as a function of deposition time is shown in figure 3(b), and the F(1*s*)-to-C(1*s*) ratio, corrected for the relative sensitivities of these two peaks, is given in figure 3(c). Fluorine uptake appears similar to the fluorocarbon film deposition, but the F-to-C plot in figure 3(c) highlights a high initial incorporation of F into the underlying SiO₂. During the O₂ plasma beam cleaning of the as-received samples (which uses the Ar⁺ ICP source), trace fluorine (resulting from cross contamination of that source) is released and leads to some initial fluorination of the SiO₂ film.

Pulsed-power deposition allows a more precise dosing for very thin films, as well as possibly offering a different relative makeup of impinging reactants that could in turn affect film growth. C(1*s*) spectra in figures 4(a) and (b) for 2.2 Å and 4.2 Å thick films are very similar to each other and to those deposited from continuous wave plasmas. F(1*s*) spectra for these two films are given in figure 4(c). Both peaks occur at nearly the same binding energy, which is slightly higher than that of SiF_{*x*}. With these very thin FC films, most of the F(1*s*)

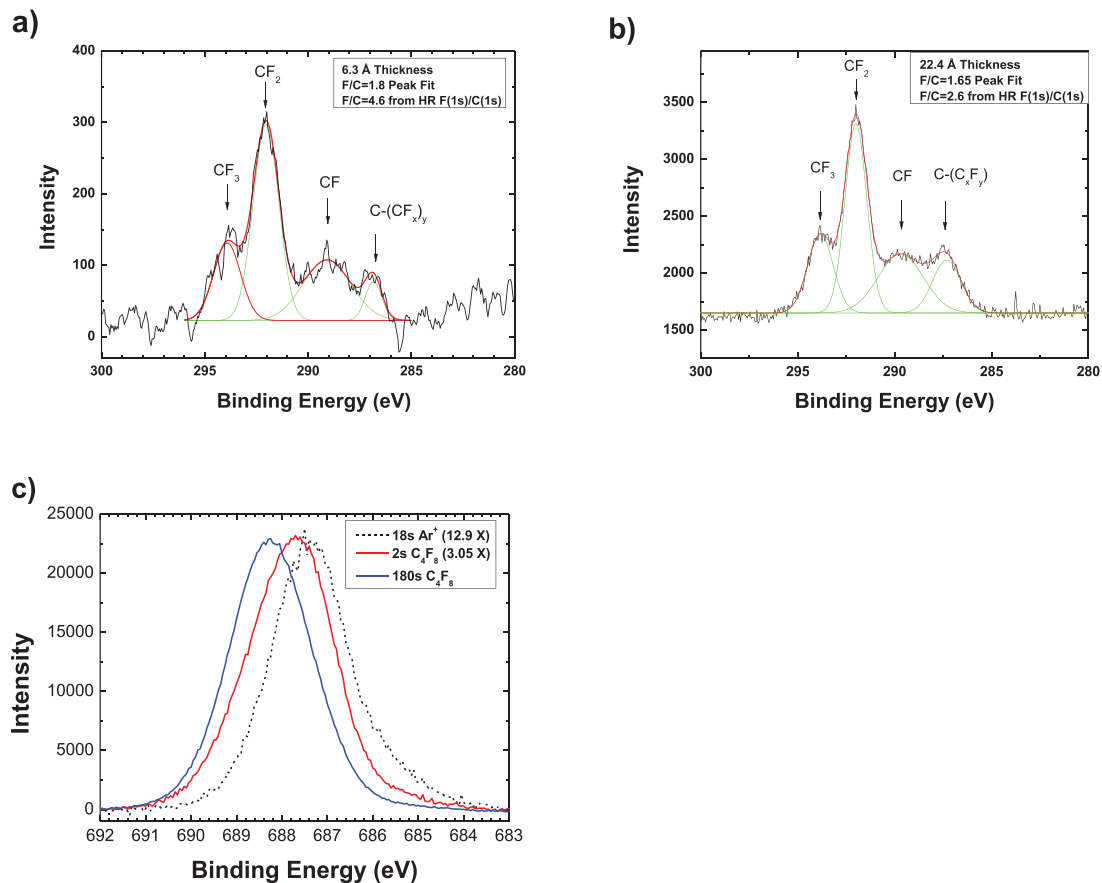


Figure 2. High resolution XPS spectra of the C(1s) region after growth of: (a) a thin (6.3 Å) and (b) a thick (22.4 Å) fluorocarbon film. (c) High resolution XPS spectra of the F(1s) region for the thin and thick films. Fresh substrates were cleaned in an O₂ plasma beam and then exposed to a 50 W continuous wave C₄F₈ plasma beam for 2 s or 180 s to grow the thin and thick films, respectively. The dotted line spectrum in figure 2(c) was recorded after 18 s Ar⁺ ion bombardment following FC film growth.

signal is coming from the fluorination of the SiO₂ film during the O₂ plasma cleaning process.

Results of fluorocarbon film deposition as a function of C₄F₈ pulsed plasma beam exposure time are shown in figure 5. Fresh samples were cleaned in an O₂ plasma beam to remove the as-received hydrocarbon contamination and then exposed to an ion beam extracted from an Ar, O₂/Ar or O₂ plasma, before exposure to a C₄F₈ pulsed plasma beam. Fluorocarbon uptake measurements are shown in figure 5(a). Pre-exposure to the 130 eV Ar⁺ beam leads to the largest uptake of the fluorocarbon film. Apparently, energetic ion bombardment creates added sites for chemisorption of CF_x and F. The least amount of deposition was found when the preconditioning was performed with a pure O₂ plasma beam. Adding 2% O₂ to the Ar plasma beam feed gas reduces the deposited film thickness by ~25%; applying a small negative bias (−15 V) to the substrate holder causes a small added reduction in thickness.

Atomic F concentration and F-to-C ratios are given in figures 5(b) and (c), respectively. As in the case of cw C₄F₈ ICP, pulsed power deposition results in an initially large amount of F that is mainly incorporated into the SiO₂ film. In particular, the low energy O₂ plasma beam pretreatment leads to the largest initial uptake of F relative to C.

The dosing time in figures 5(a)–(c) is total time, including the power-off portion of the cycle, but since the duty cycle was 50%, the true dosing time could be half the *x*-axis values shown. The apparently thinner layer for pulsed power operation, compared with the cw case in figures 3(a)–(c) could be, at least in part, due to this uncertainty in the scaling of cw and pulsed plasma dosing times. Another cause could be the relative lack of ion bombardment in the cw case. It was found that positive ion beams extracted from a continuously powered plasma suffer from Coulomb explosion, resulting in very few ions reaching a substrate. When the plasma was pulsed, however, the beam was apparently neutralized by a flux of electrons into the beam and much higher ion fluxes were found to reach the substrate [31]. This would suggest that positive ion bombardment may suppress deposition somewhat.

Sawin and co-workers studied ion-assisted etching of SiO₂ by simultaneously exposing the substrate to an effusive CF₂ neutral flux and an energetic Ar⁺ ion beam [32]. The etching yield increased by increasing ion energy or CF₂-to-Ar⁺ flux ratio. For high flux ratios, the yield saturated at ~0.3 for 150 eV Ar⁺ ions. Yield saturation implies that CF₂ forms a saturated FC layer on SiO₂. If this were not the case, and the CF₂ sticking coefficient on the FC layer were comparable to that on SiO₂, then the yield would continue to increase to a maximum value as a function of CF₂-to-Ar⁺ ratio, and then the yield would

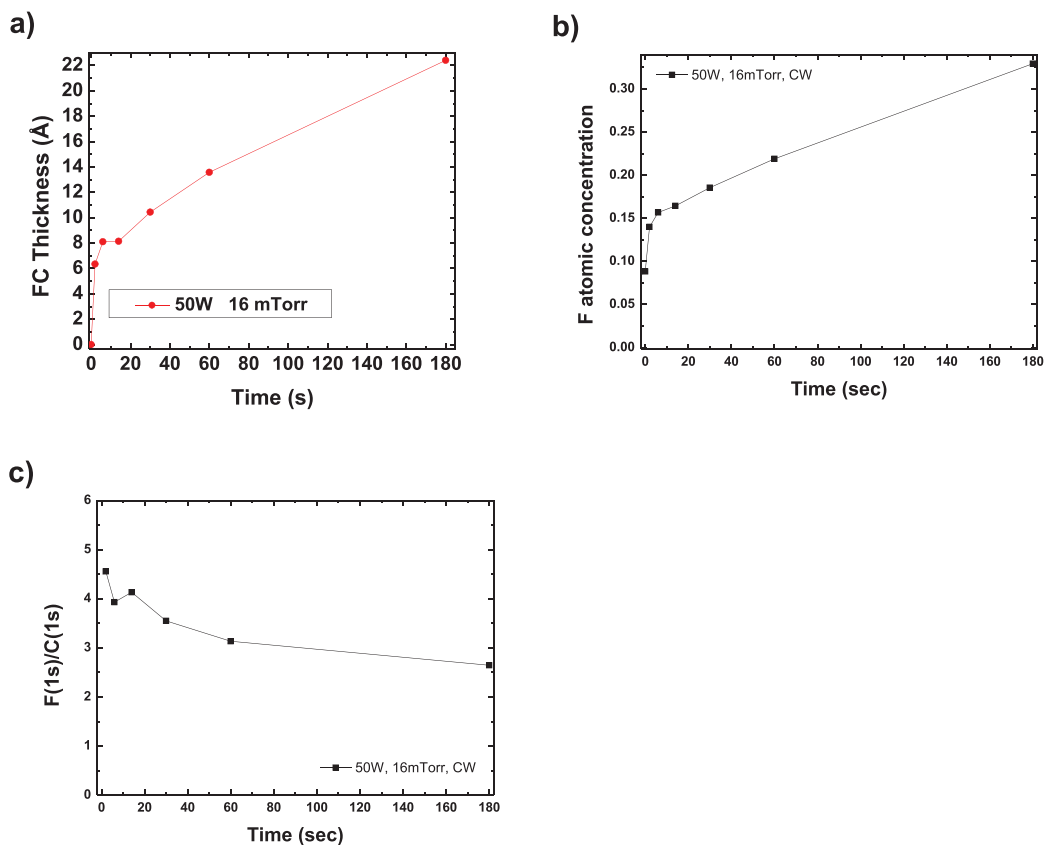


Figure 3. (a) Fluorocarbon film thickness versus plasma beam exposure time using a 16 mTorr, 50 W continuous wave $c\text{-C}_4\text{F}_8$ plasma. The gas flow rate was 10 sccm. (b) Atomic fluorine concentration, integrated over the deposited layer and SiO_2 film, uncorrected for decreasing signal as a function of depth. (c) F-to-C ratios derived from the F(1s) and C(1s) integrated peak intensities, corrected for the relative sensitivity factors.

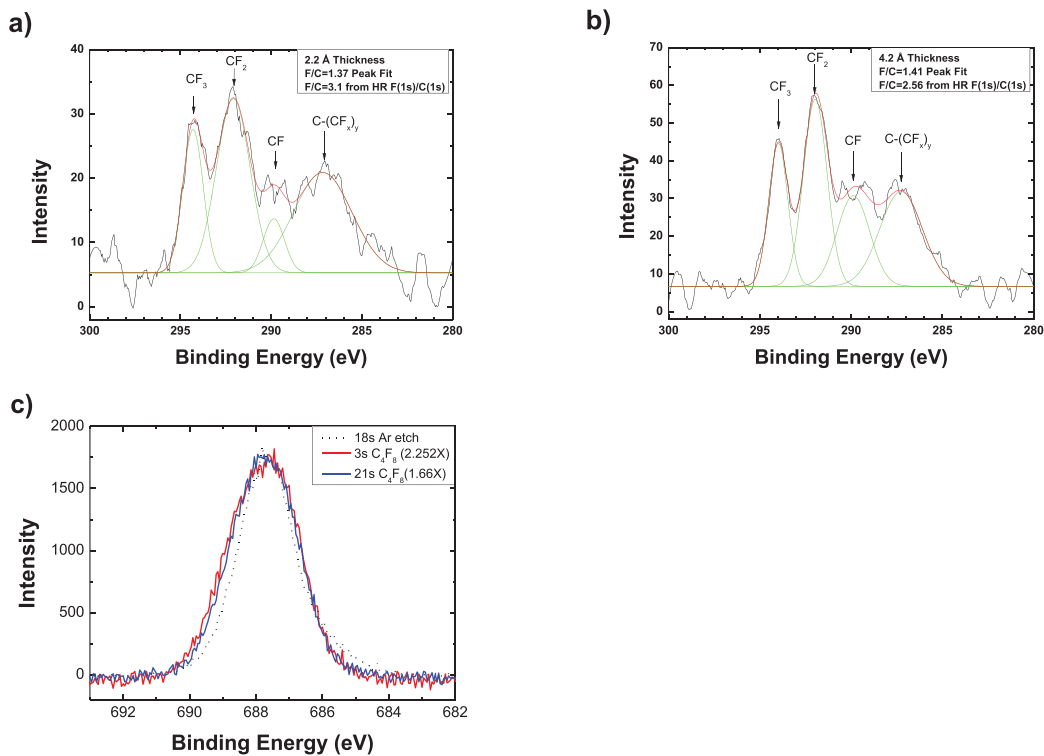


Figure 4. High resolution XPS spectra of the C(1s) region after growth of (a) a thin (2.2 Å) and (b) a thick (4.2 Å) fluorocarbon film. (c) High resolution XPS spectra of the F(1s) region for the thin and thick films. Fresh substrates were cleaned in an O_2 plasma beam and then exposed to a 130 eV Ar^+ beam before exposure to a 50 W pulsed C_4F_8 plasma beam (10 kHz, 50% duty cycle) for 3 s or 21 s to grow the thin and thick films, respectively.

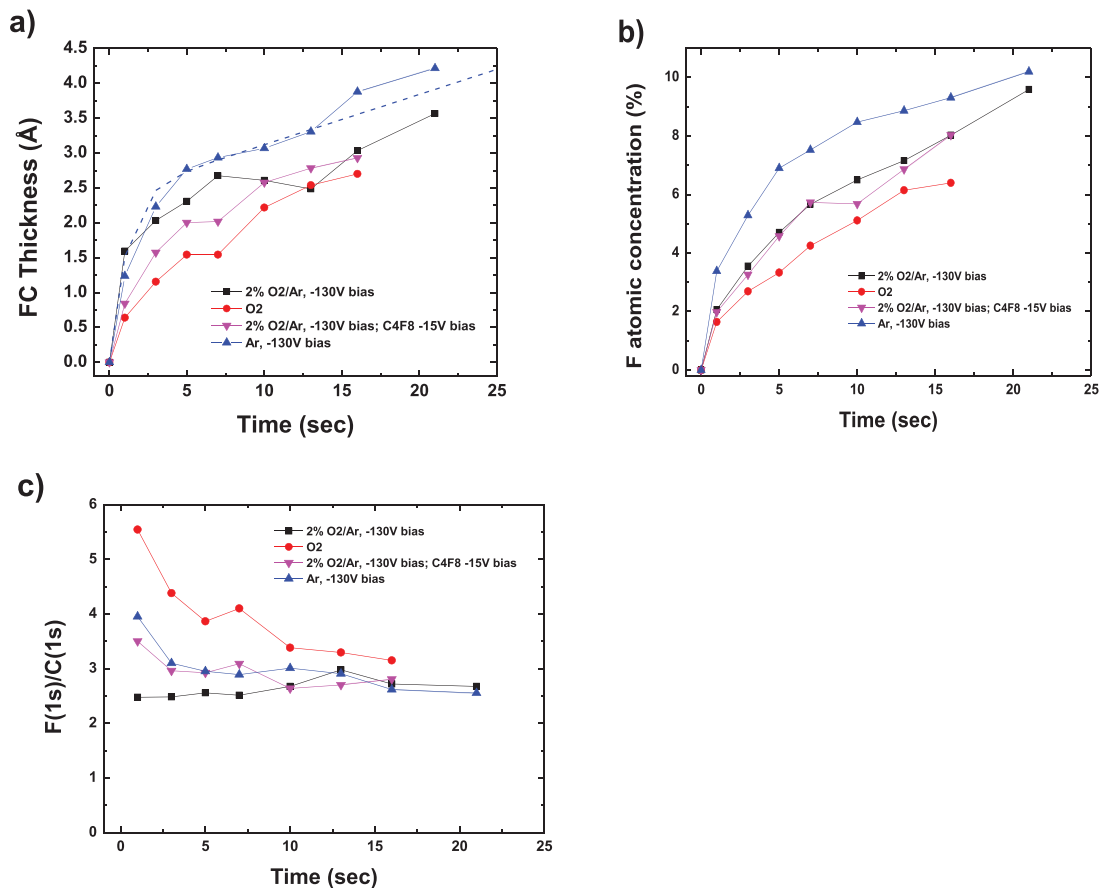


Figure 5. (a) Fluorocarbon film thickness versus plasma beam exposure time (the sum of power on and off times) using a 10 mTorr, 50 W (peak power) pulsed *c*-C₄F₈ plasma (10kHz, 50% duty cycle). The gas flow rate was 10 sccm. The dotted line is a model fit (see text). (b) Atomic fluorine concentration, integrated over the deposited layer and SiO₂ film, uncorrected for decreasing signal as a function of depth. (c) F-to-C ratios derived from the F(1s) and C(1s) integrated peak intensities, corrected for the relative sensitivity factors. Fresh substrates were cleaned in an O₂ plasma beam, exposed to one of the surface treatments given in the figure, and then to the C₄F₈ plasma beam.

decrease to zero as the FC film became thick enough to prevent ions and ion-activated reactants (e.g. F-atoms) in the FC film from reaching the film/oxide interface. In addition, there is evidence that CF₂ chemisorbs on SiO₂, forming a monolayer [33]. CF₂ does not ‘stick’ efficiently on the chemisorbed layer, hence a very thin FC film should achieve a self-limiting thickness upon exposure of SiO₂ to excess of CF₂.

In measurements described elsewhere [34], we found that the *c*-C₄F₈ plasma contains mostly CF₂ in a 10kHz, 50% duty cycle pulsed plasma at peak powers >150 W. Furthermore, the CF₂ number density remained nearly constant between 150 W and 450 W peak power. The plasma will likely also contain a large amount of C₂F₄, particularly relative to CF₂ at lower powers where the CF₂ number density is rising steeply. It has been reported [33] that C₂F₄ does not stick to SiO₂, however, so it is not expected to play a role in the ALE mechanism. Since the CF number density is very low (barely detectable by UV absorption at the highest power), and CF/CF₂ number density will decrease rapidly with decreasing power, it is not likely that CF is very important; hence CF₂ is the only viable deposition precursor in the present study.

Using the measured, time-averaged number density of $1.6 \times 10^{13} \text{ cm}^{-3}$ in a 50 W peak power pulsed plasma, we estimate a time-averaged CF₂ flux of $5 \times 10^{15} \text{ cm}^{-2} \text{ s}^{-1}$ at the substrate surface. Sawin and co-workers derived a

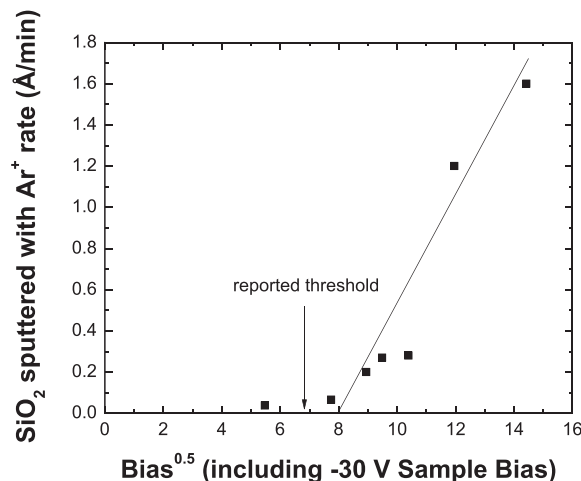


Figure 6. SiO₂ sputtering rate under Ar⁺ ion bombardment. Each data point was measured after 10 min exposure to an Ar⁺ ion beam, extracted from a pulsed plasma in Ar gas (10kHz, 20% duty cycle, 600 W peak power) with a boundary electrode bias applied during the afterglow. The sample holder was biased at -30 V. A fresh 5 nm SiO₂-on-Si sample, cleaned with an O₂ plasma beam, was used for each data point. A SiO₂ sputtering rate of 1.6 Å min^{-1} was measured with 170 V boundary electrode bias (200 V total bias). With no boundary electrode bias applied (i.e. with only the sample holder bias), the SiO₂ sputtering rate was almost completely suppressed.

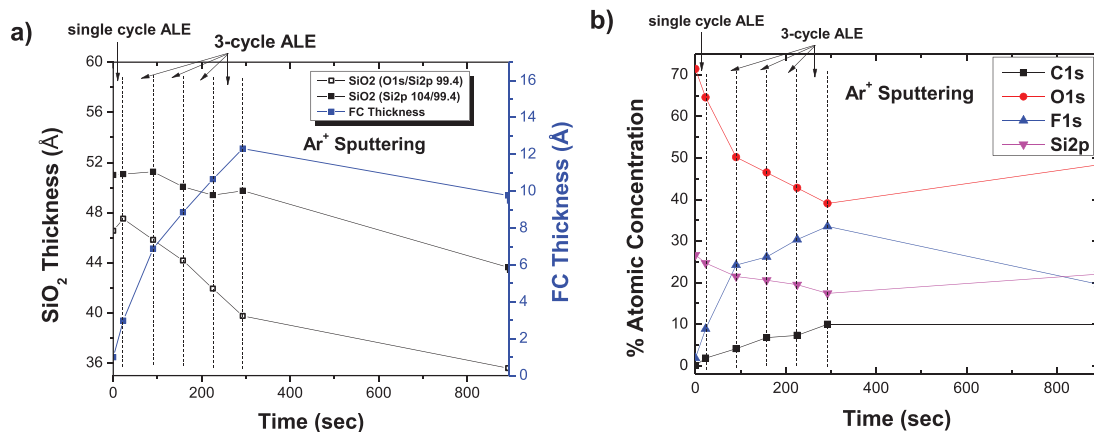


Figure 7. (a) SiO₂ and fluorocarbon film thickness versus time; (b) atomic concentrations of C(1s), O(1s), F(1s) and Si(2p) versus time. Data was collected after the first ALE cycle and after each of the four sets, with a three-cycle ALE in each set. An ALE cycle consisted of 2.5 s C₄F₈ 10 kHz, 50% duty cycle pulsed plasma at 50 W peak power, and a 20 s exposure to a 90 eV Ar⁺ beam. The last data point corresponds to continuous sputtering (starting at 293 s and ending at 893 s) with 90 eV Ar⁺.

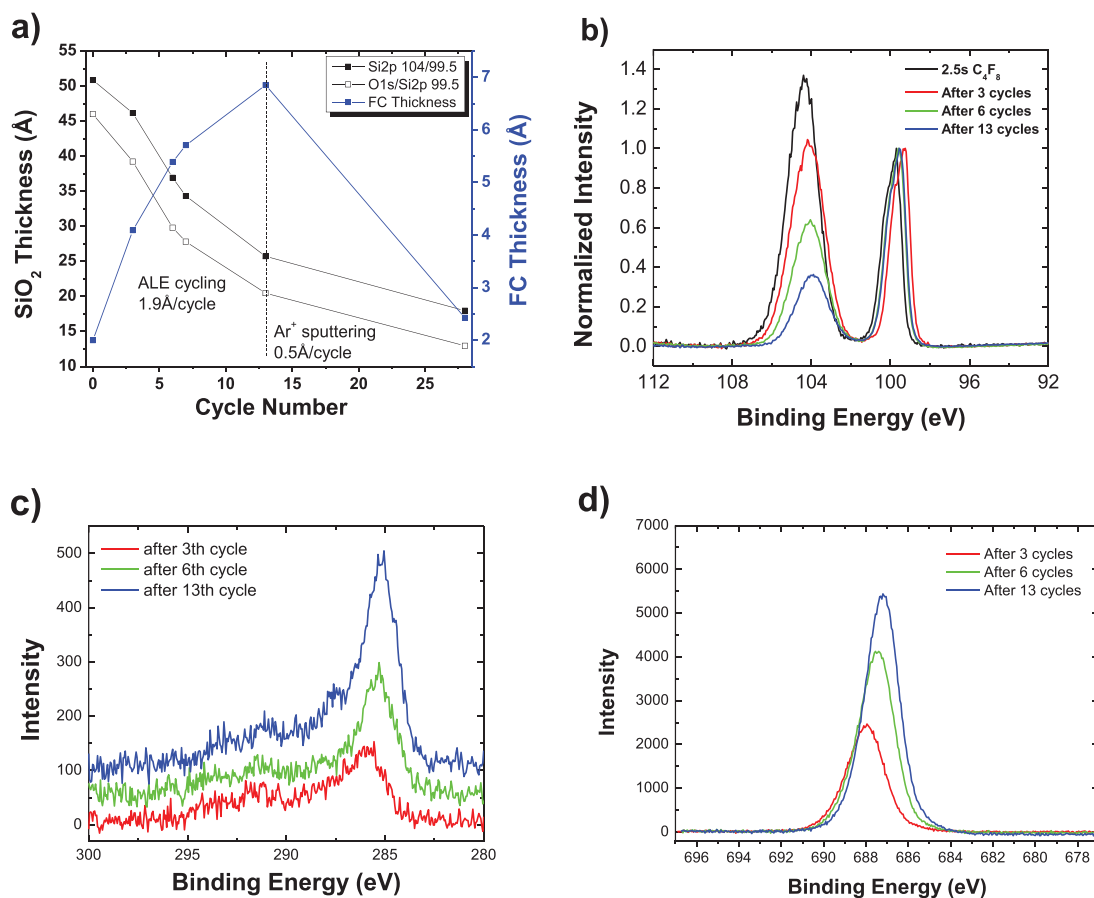


Figure 8. (a) SiO₂ and fluorocarbon film thickness versus ALE cycle number. Two methods were used to estimate the oxide thickness (see text). (b) XPS high resolution spectra of the Si(2p) region after 2.5 s of FC film growth of the first ALE cycle, and after the end of 3, 6 and 13 ALE cycles. (c) XPS high resolution spectra of the C(1s) region after the end of 3, 6 and 13 ALE cycles (intensities offset by 200, 250 and 300 for clarity). (d) XPS high resolution spectra of the F(1s) region after the end of 3, 6 and 13 ALE cycles. An ALE cycle consisted of a 2.5 s c-C₄F₈ pulsed plasma exposure (FC film growth), followed by 20 s of 130 eV Ar⁺ ion bombardment.

sticking coefficient of 0.19 for CF₂ on SiO₂ during etching with CF₂ and 150 eV Ar⁺ beams [33]. Fisher and co-workers reported that CF₂ has a very small sticking probability on poly-tetrafluoro-ethylene (PTFE). They measured a reflection coefficient (1 - s_{FC}, where s_{FC} is the sticking coefficient on the fluorocarbon film) of 1.06 ± 0.09. Assuming a simple

Langmuir–Hinshelwood model for adsorption of CF₂ to form a fluorocarbon layer of thickness h_{FC}(t), a site density of S on SiO₂ or the FC film surface on which irreversible adsorption of CF₂ can occur, a sticking coefficient s_{ox} for CF₂ on bare sites on SiO₂ and a sticking coefficient s_{FC} for CF₂ on the FC film, then the depositing film thickness is given by

$$h^{\text{tot}}(t) = h_0 \left(1 - \exp \left[-\frac{f_{\text{CF}_2} s_{\text{ox}}}{S} t \right] \right) \left(1 + \frac{f_{\text{CF}_2} s_{\text{FC}}}{S} t \right).$$

The dashed line in figure 5(a) is a predicted thickness versus time, using the estimated CF_2 flux, with $S = 1 \times 10^{15} \text{ cm}^{-2}$, $s_{\text{ox}} = 0.19$, and adjustable parameters $s_{\text{FC}} = 0.015$ and $h_0 = 2.4 \text{ \AA}$. The derived sticking coefficient for CF_2 on the growing film is well within the uncertainty of the value measured by Fisher and co-workers, while the thickness of a monolayer of the film is close to but less than that for bulk PTFE (3.3 \AA).

3.2. Ar^+ ion bombardment of fluorocarbon-dosed surfaces

Following deposition of a pseudo-saturated FC film, the sample was bombarded with an Ar^+ ion beam to complete an ALE cycle. Before presenting these results, sputtering measurements are shown in figure 6 for SiO_2 surfaces that are free of FC films. The ion energy was equal to the boundary electrode bias plus the absolute value of the substrate bias. No sputtering was observed until reaching a threshold energy of $\sim 65 \text{ eV}$. This is in excess of the reported threshold of $\sim 45 \text{ eV}$ [4]. Perhaps a voltage drop occurring across the 50 \AA thick SiO_2 film can explain this discrepancy.

ALE was investigated at Ar^+ beam energies of 90 and 130 eV. Two methods of SiO_2 thickness change were used to determine the etching rate per cycle. Figure 7(a) presents measurements for 90 eV Ar^+ . The $\text{O}(1s)$ -to- $\text{Si}(2p)$, (substrate) ratio yielded an apparent etching rate of $\sim 0.6 \text{ \AA/cycle}$. The $\text{Si}(2p, \text{SiO}_2)$ -to- $\text{Si}(2p)$, (substrate) ratio, however, gave a much lower apparent etching rate of 0.09 \AA/cycle . Since fluorinated Si has a $2p$ binding energy about the same as SiO_2 , this suggests that instead of etching, O in the SiO_2 film was being displaced by F in an ion-stimulated reaction, and that little removal of the fluorinated film occurred. This was confirmed by the atomic concentration measurements as a function of Ar^+ exposure (figure 7(b)) in which the drop in O is mirrored by a rise in F.

Raising the Ar^+ beam energy to 130 eV produced a very different result. As shown in figures 8(a) and (b), etching was confirmed by the nearly identical change in SiO_2 thickness obtained by the two methods. An etching rate of 1.9 \AA/cycle was found after 13 cycles. At this point the sample was continuously exposed to the Ar^+ beam for a period of 300 s, which corresponds to 15 ALE cycles. The thickness change over this time was then converted to an equivalent sputtering rate of 0.5 \AA/cycle , or about 1/4 of the ALE rate with alternating exposure to the C_4F_8 plasma beam. Since there was still appreciable fluorine and carbon on the surface during this sputtering process, the 0.5 \AA/cycle value is an upper limit to the true sputtering rate.

In several cases, XPS measurements were carried out for a thin FC film that was exposed to the Ar^+ beam for increasing times. In the example in figure 9, a 6.2 \AA -thick FC film was deposited (pulsed C_4F_8 plasma, 50 W, 10 kHz, 50% duty cycle) for 2.5 s and then exposed to the 130 eV Ar^+ beam for periods of 1, 1, 2, 4, 4 and 4 s to complete one ALE cycle.

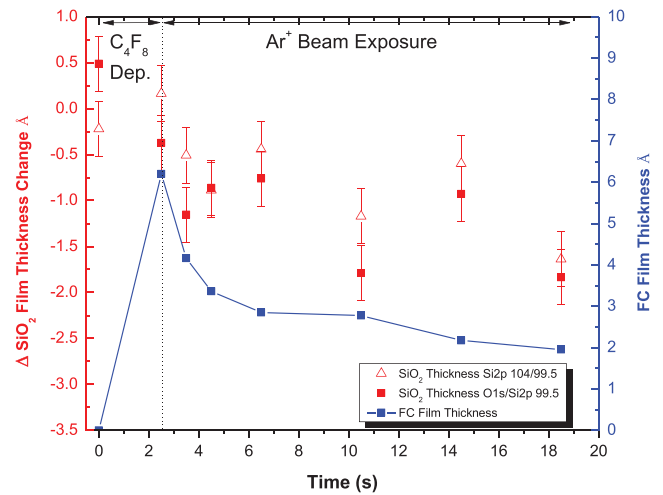


Figure 9. SiO_2 and fluorocarbon film thickness for a single ALE cycle, consisting of 2.5 s C_4F_8 plasma exposure (FC film growth) followed by Ar^+ ion (130 eV) bombardment for 1 s, 1 additional s, 2 additional s, 4 additional s, 4 additional s, and 4 additional s, each processing step followed by XPS analysis. Two methods were used to estimate the oxide thickness (see text).

XPS analysis was performed after each period of Ar^+ exposure. The change in SiO_2 thickness determined from both the $\text{O}(1s)$ -to- $\text{Si}(2p)$, (substrate) and $\text{Si}(2p, \text{oxide})$ -to- $\text{Si}(2p)$, (substrate) intensity ratios are in agreement within the uncertainty of the measurement, and correspond to the removal of about 1.6 \AA of SiO_2 . The FC film was mostly consumed in this process, leaving a 2 \AA thick residue. The 1.6 \AA of SiO_2 removed in one cycle in figure 9 corresponds to 0.5 monolayers of SiO_2 per cycle or roughly $4 \times 10^{14} \text{ SiO}_2 \text{ cm}^{-2}$. In the 16 s that this took, the Ar^+ dose was about $3 \times 10^{14} \text{ cm}^{-2}$. This suggests a yield of roughly 1.3 SiO_2 molecules/ion. Sawin and co-workers reported yields of about 0.3 for continuous CF_2 and Ar^+ beams and 0.6 for F and Ar^+ beams at a somewhat higher Ar^+ beam energy of 150 eV. Thus, the yields in the present study are perhaps a little high, but not unreasonable.

Figure 10(a) presents $\text{C}(1s)$ spectra as a function of Ar^+ dosing time that were used to determine the thickness change measurements in figure 9. During Ar^+ bombardment, the FC layer is transformed from a layer rich in CF_2 and CF_3 into one with a majority of F-deficient CF and $\text{C}-(\text{CF}_x)\text{F}_y$. This is in good agreement with previously published ALE SiO_2 studies [4, 23, 24, 35]. In addition, some residual F bound mostly to Si is present in the near surface region, as seen in the $\text{F}(1s)$ spectra in figure 10(b). An increasingly thick layer of this carbon-rich residue was left on the surface with increasing number of ALE cycles (figures 8(b) and (c)). Despite this, the ALE rate seems to be constant, within the uncertainty of the measurement. Nonetheless, it would be desirable to remove this carbon-rich residue.

A small amount (2%) of O_2 was added to the Ar ICP used for the Ar^+ ion beam exposure step, to attempt to suppress buildup of the carbon residue. This indeed slows the carbon buildup (figure 11), but also slows the ALE rate to $\sim 0.4 \text{ \AA/cycle}$. Adding 20% O_2 to the Ar^+ beam eliminated the carbon-rich residue, but also stopped etching of SiO_2 . This may still not be a problem. One reasonable approach would be to carry out about 10 ALE

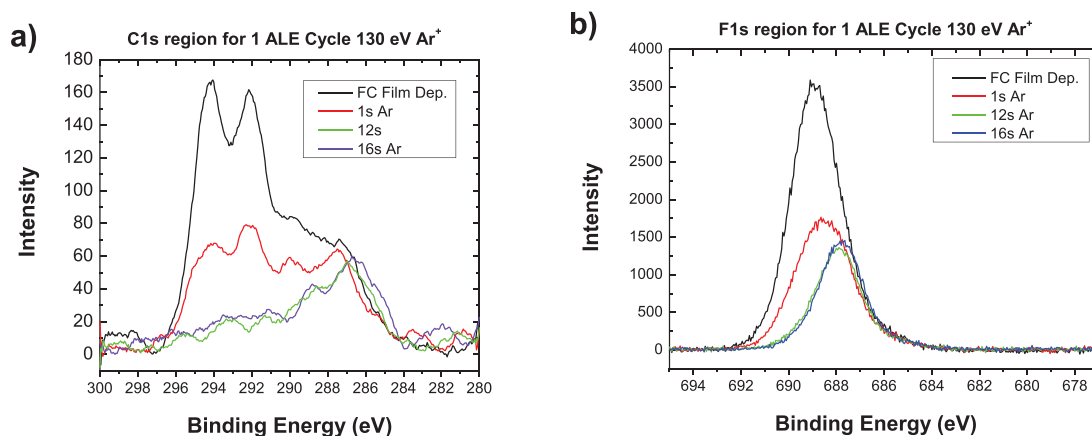


Figure 10. XPS high resolution spectra of (a) C(1s); (b) F(1s) regions after 2.5 s of FC film growth and after 1 s, 12 s, and 16 s Ar⁺ ion (130 eV) bombardment.

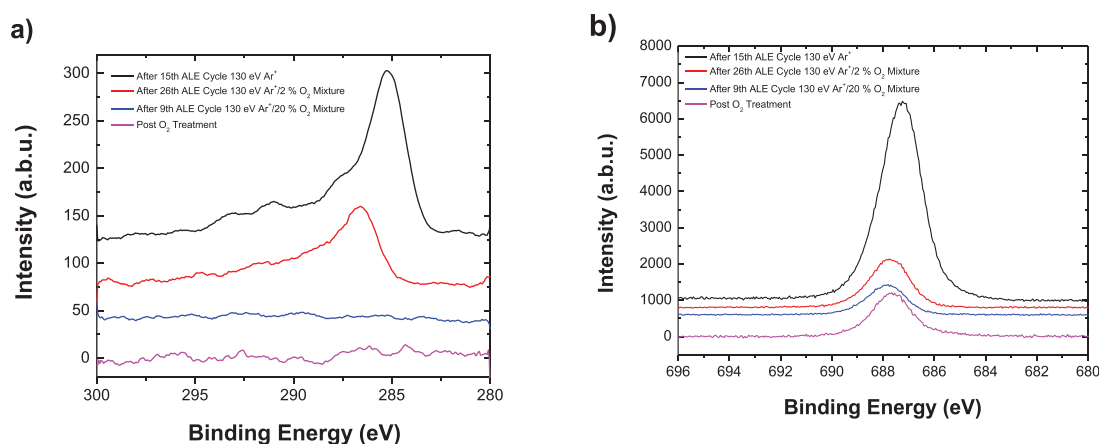


Figure 11. XPS high resolution spectra of (a) C(1s); (b) F(1s) regions after 15 ALE cycles with 130 eV Ar⁺ bombardment, after 26 ALE cycles with 130 eV Ar⁺/2% O₂ mixture, after 9 ALE cycles with 130 eV Ar⁺/20% O₂ mixture, or after pure O₂ plasma clean. An ALE cycle consisted of a 2.5 s c-C₄F₈ pulsed plasma exposure (FC film growth), followed by 20 s of 130 eV ion beam bombardment.

cycles with an Ar⁺ beam with no added O₂ and then expose the surface to a 20% O₂/Ar⁺ beam before continuing with more ALE cycles. Alternatively, a pure O₂ plasma beam with no bias voltages applied could be used to periodically remove the carbon residue (figure 11). Tsutsumi *et al* developed an ALE SiO₂ process where O₂ plasma irradiation was used as the modified layer removal step, following fluorocarbon film deposition. They successfully suppressed a carbon-rich residual film while removing a consistent amount of SiO₂ per cycle [35].

In comparison to references [4, 23], a similar SiO₂ etch rate was measured. However, the Ar⁺ beam ion energies in our study were much larger, and little or no etching was found at lower energies. While this discrepancy is somewhat puzzling, at least some of the difference could be due to the maximum ion energy being somewhat higher than stated in Metzler *et al*'s work due to an RF component to the plasma potential in ICP plasmas.

4. Summary and conclusions

Atomic layer etching (ALE) of SiO₂ was developed by alternating exposure of a substrate to (1) a CF₂-rich plasma beam, emanating from a c-C₄F₈ inductively coupled plasma (ICP), to

grow a fluorocarbon (FC) film composed mainly of CF₂, and (2) an energetic Ar⁺ ion beam extracted from a separate ICP in Ar to etch a self-limited amount of SiO₂. *In situ* x-ray photoelectron spectroscopy (XPS) was used to analyze the chemical composition of the near surface region and to quantify the thickness of the FC and SiO₂ films. 'As received' samples were initially exposed to an O₂ plasma beam, to remove residual carbon contamination. A near-self-limiting FC film thickness of ~8 Å occurred, after a relatively brief exposure to the C₄F₈ plasma beam, followed by a much slower, continuous deposition of a FC film with very similar composition. This behavior was explained by a relatively high sticking coefficient of CF₂ on SiO₂, combined with a much lower sticking coefficient of CF₂ on the growing FC film. A modified Langmuir–Hinshelwood model predicted the FC uptake.

Multiple ALE cycles were performed with each cycle consisting of a brief (typically several s) exposure to the C₄F₈ plasma beam to deposit a pseudo-saturated FC film, followed by 20 s exposure to a 130 eV Ar⁺ beam. Over 13 ALE cycles, an etching rate of 1.9 Å/cycle was measured. Lowering the Ar⁺ energy to 90 eV resulted in fluorination of the SiO₂ film, but little etching. From the measured Ar⁺ flux, a yield of roughly 1.3 SiO₂ molecules etched per incident

130 eV Ar⁺ was obtained. In addition to removing SiO₂ etching products, Ar⁺ bombardment decomposed the CF₂ and CF₃ components in the FC layer, leading to a build-up of a C-rich layer and fluorination of the SiO₂ layer. The growth of such residual film would ultimately halt SiO₂ etching. This film, however, can be periodically removed by briefly exposing the surface to an oxygen-rich beam, allowing uninterrupted etching of SiO₂.

Acknowledgments

Financial support for this work was provided by Lam Research, the National Science Foundation grant PHY-1500518, and the Department of Energy, Office of Fusion Energy Science, contract DE-SC0001939. The authors are grateful to Dr Meihua Shen and Dr Eric Hudson, both of Lam Research, for many fruitful technical discussions.

References

- [1] Donnelly V M and Kornblit A 2013 Plasma etching: yesterday, today, and tomorrow *J. Vac. Sci. Technol. A* **31** 050825
- [2] Lee C G N, Kanarik K J and Gottscho R A 2014 The grand challenges of plasma etching: a manufacturing perspective *J. Phys. D: Appl. Phys.* **47** 273001
- [3] Kanarik K J, Lill T, Hudson E A, Sriraman S, Tan S, Marks J, Vahedi V and Gottscho R A 2015 Overview of atomic layer etching in the semiconductor industry *J. Vac. Sci. Technol. A* **33** 020802
- [4] Oehrlein G S, Metzler D and Li C 2015 Atomic layer etching at the tipping point: an overview *ECS J. Solid State Sci. Technol.* **4** 5041
- [5] Yoder M N 1988 Atomic layer etching *Google Patents* US4756794 A
- [6] Meguro T, Hamagaki M, Modaressi S, Hara T and Aoyagi Y 1990 Digital etching of GaAs: new approach of dry etching to atomic ordered processing *Appl. Phys. Lett.* **56** 1552
- [7] Aoyagi Y, Shinmura K, Kawasaki K, Tanaka T, Gamo K, Namba S and Nakamoto I 1992 Molecular layer etching of GaAs *Appl. Phys. Lett.* **60** 968
- [8] Ishii M, Meguro T, Kodama H, Yamamoto Y and Aoyagi Y 1992 Study of surface processes in the digital etching of GaAs *Japan. J. Appl. Phys.* **31** 2212
- [9] Aoyagi Y, Shinmura K, Kawasaki K, Nakamoto I, Gamo K and Namba S 1993 Atomic layer manipulation of III–V compounds *Thin Solid Films* **225** 120
- [10] Meguro T, Ishii M, Kodama K, Yamamoto Y, Gamo K and Aoyagi Y 1993 Surface processes in digital etching of GaAs *Thin Solid Films* **225** 136
- [11] Bourne O L, D'Arcy Hart, Rayner D M and Hackett P A 1993 Digital etching of III–V multilayered structures combined with laser ionization mass spectroscopy: photon-assisted depth profiling *J. Vac. Sci. Technol. B* **11** 556
- [12] Ishii M, Meguro T, Gamo K, Sugano T and Aoyagi Y 1993 Digital etching using KrF excimer laser: approach to atomic-order-controlled etching by photo induced reaction *Japan. J. of Appl. Phys.* **32** 6178
- [13] Horiike Y, Tanaka T, Nakano M, Iseda S, Sakaue H, Nagata A, Shindo H, Miyazaki S and Hirose M 1990 Digital chemical vapor deposition and etching technologies for semiconductor processing *J. Vac. Sci. Technol. A* **8** 1844
- [14] Park S D, Lee D H and Yeom G Y 2005 Atomic layer etching of Si(100) and Si(111) using Cl₂ and Ar neutral beam *Electrochem. Solid-State Lett.* **8** C106
- [15] Athavale S and Economou D J 1995 Molecular dynamics simulation of atomic layer etching (ALET) of silicon *J. Vac. Sci. Technol. A* **13** 966
- [16] Athavale S and Economou D J 1996 Realization of atomic layer etching (ALET) of silicon *J. Vac. Sci. Technol. B* **14** 3702
- [17] Lee Y H and Chen M M 1986 Silicon doping effects in reactive plasma etching *J. Vac. Sci. Technol. B* **4** 468
- [18] Zhu W, Sridhar S, Liu L, Hernandez E, Donnelly V M and Economou D J 2014 Photo-assisted etching of silicon in chlorine- and bromine-containing plasmas *J. Appl. Phys.* **115** 203303
- [19] Tan S, Yang W, Kanarik J K, Thorsten L, Vahedi V, Marks J and Gottscho R A 2015 Highly selective directional atomic layer etching of silicon *ECS J. Solid State Sci. Technol.* **4** 5010
- [20] Sherpa S D and Ranjan A 2017 Quasi-atomic layer etching of silicon nitride *J. Vac. Sci. Technol. A* **35** 01A102
- [21] Rauf S, Sparks T, Ventzek P L G, Smirnov V V, Stengach A V, Gaynullin K G and Pavlovsky V A 2007 A molecular dynamics investigation of fluorocarbon based layer-by-layer etching of silicon and SiO₂ *J. Appl. Phys.* **101** 033308
- [22] Agarwal A and Kushner M J 2009 Plasma atomic layer etching using conventional plasma equipment *J. Vac. Sci. Technol. A* **27** 37
- [23] Metzler D, Bruce R L, Engelmann S, Joseph E A and Oehrlein G S 2014 Fluorocarbon assisted atomic layer etching of SiO₂ using cyclic Ar/C₄F₈ plasma *J. Vac. Sci. Technol. A* **32** 020603
- [24] Li C, Metzler D, Lai C S, Hudson E A and Oehrlein G S 2016 Fluorocarbon based atomic layer etching of Si₃N₄ and etching selectivity of SiO₂ over Si₃N₄ *J. Vac. Sci. Technol. A* **34** 041307
- [25] Shin H, Zhu W, Xu L, Ouk T, Economou D J and Donnelly V M 2011 Control of ion energy distributions using a pulsed plasma with synchronous bias on a boundary electrode *Plasma Sources Sci. Technol.* **20** 055001
- [26] Donnelly V M, Klemens F P, Sorsch T W, Timps G L and Baimann F H 1999 Oxidation of Si beneath thin SiO₂ layers during exposure to HBr/O₂ plasmas, investigated by vacuum transfer x-ray photoelectron spectroscopy *Appl. Phys. Lett.* **74** 1260
- [27] Seah M P and Dench W A 1979 Quantitative electron spectroscopy of surfaces: a standard data base for electron inelastic mean free paths in solids *Surf. Interface Anal.* **1** 2
- [28] Pelhos K, Donnelly V M, Kornblit A, Green M L, Van Dover R B, Manchanda L, Hu Y, Morris M and Bower E 2001 Etching of high-*k* dielectric Zr_{1-x}Al_xO_y films in chlorine-containing plasmas *J. Vac. Sci. Technol. A* **19** 1361
- [29] Wagner C D, Riggs W M, Davis L E, Moulder J F and Muilenberg G E 1979 *Handbook of X-Ray Photoelectron Spectroscopy* (Eden Praire, MN: Perkin-Elmer, Physical Electronics Division)
- [30] Limb S J, Labelle C B and Gleason K K 1996 Growth of fluorocarbon polymer thin films with high CF₂ fractions and low dangling bond concentrations by thermal chemical vapor deposition *Appl. Phys. Lett.* **68** 2810
- [31] Tian S 2015 Sub 10 nm nanopantography and nanopattern transfer using highly selective plasma etching *PhD Thesis* University of Houston
- [32] Butterbaugh J W, Gray D C and Sawin H H 1991 Plasma-surface interactions in fluorocarbon etching of silicon dioxide *J. Vac. Sci. Technol. B* **9** 1461
- [33] Langan J G, Shorter J A, Xin X, Joyce S A and Steinfield J I 1989 Reactions of laser-generated CF₂ on silicon and silicon oxide surfaces *Surf. Sci.* **207** 344
- [34] Lou Q, Kaler S S, Donnelly V M and Economou D J 2016 unpublished
- [35] Tsutsumi T, Kondo H, Zaitzu M H, Kobayashi A, Nozawa T and Kobayashi N 2017 Atomic layer etching of SiO₂ by alternating an O₂ plasma with fluorocarbon film deposition *J. Vac. Sci. Technol. A* **35** 01A103